Thermophoresis in Dense Gases : a Study by Born-Green-Yvon Equation

Minsub Han*

Micro Thermal System Research Center, Seoul National University, San 56-1, Shinlim-dong, Kwanak-gu, Seoul 151-742, Korea

Thermophoresis in dense gases is studied by using a multi-scale approach and Born-Yvon-Green (BYG) equation. The problem of a particle movement in an ambient dense gas under temperature gradient is divided into inter and outer ones. The pressure gradient in the inner region is obtained from the solutions of BYG equation. The velocity profile is derived from the conservation equations and calculated using the pressure gradient, which provides the particle velocity in the outer problem. It is shown that the temperature gradient applied to the quiescent ambient gas induces some pressure gradient and thus flow tangential to the particle surface in the interfacial region. The mechanism that induces the flow may be the dominant source of the thermophretic particle movement in dense gases. It is also shown that the particle velocity has a nonlinear relationship with the applied temperature gradient and decreases with increasing temperature.

Key Words: Colloid, YBG Equation, Thermoosmosis

Nomenclature

A : Force constant of graphite basal plane
A_C : Effective cross-sectional area of collision
a : Radius of particle
a_s : Area of unit lattice cell of graphite basal plane
d : Equivalent hard sphere diameter
$g(\vec{r}_1, \vec{r}_2)$: Pair correlation function
$g^{HS}(r, \rho)$: Correlation function of homogeneous fluid of hard sphere
K_n : Knudsen number
k : Thermal conductivity
k_B : Boltzmann Constant
L : Distance over which unit temperature difference is applied
l : Mean free path
P : Pressure tensor
q : The total number of atoms per unit surface cell of graphite basal plane
R : Gas constant
r_i : Effective range of intermolecular force during collision
r_{12} : Distance between $\vec{r}_1$ and $\vec{r}_2$
T : Temperature
U_{th} : Thermophoretic velocity of particle
u : Velocity component in x direction
V : Spherical volume of diameter d centered at $\vec{r}$
$\tilde{X}, \tilde{Z}$: Macro-scale coordinates
x, z : Molecular-scale coordinates
Δz : Distance between discrete planes of graphite basal plane

Greek symbols

ε : Interaction energy
μ : Viscosity
ρ : Density
σ : Molecular diameter
σ_{ss} : The nearest neighbor distance of graphite
ϕ : Intermolecular potential

* **E-mail** : bard2@snu.ac.kr
TEL : +82-2-880-7123; **FAX** : +82-2-874-5129
Micro Thermal System Research Center, Seoul National University, San 56-1, Shinlim-dong, Kwanak-gu, Seoul 151-742, Korea. (Manuscript **Received** September 13, 2004; **Revised** February 17, 2005)

Subscripts

e : Equilibrium state
ff : Between fluid molecules
g : Gas
gs : Between gas and solid
o : Particle position
p : Particle
s : Solid
T : Tangential direction
$*$: Scaled with $\sqrt{3}\sigma_{ss}$

Superscripts

HS : Hard sphere
0 : The first order

1. Introduction

Thermophoresis is the phenomenon that small particles in an ambient fluid under temperature gradient move toward one end. A typical example is the collection of small particles near thermal boundary layer. It occurs irrespective of convection or gravity and is found commonly in colloidal systems. The phenomenon has importance in a wide range of applications in the fields like, for example, the cleaning process, combustion, and chemical vapor deposition.

Maxwell (1879) first suggested the origin of the phenomenon postulating the molecular interaction between the particle and fluid molecules. A particle may be under constant and random bombardments of the surrounding fluid molecules. Since the fluid molecules in hotter region would give larger impacts than those in colder, the net momentum transferred to the particle may be directed towards the colder region. A quantitative model on the phenomenon may be developed with the help of the kinetic theory of gases. Epstein (1929) derived the thermophoretic velocity for the gases of a small Knudsen number.

$$U_{th}=-\frac{3}{2}\frac{k}{2k+k_p}\frac{\mu}{\rho T}\nabla T \tag{1}$$

Since then, there have been extensive studies, both theoretical and experimental, on the subject (Sone, 2000; Zheng, 2002). They include the results in the wide range of Knudsen number, the rigorous models based on Boltzmann equation, and the particle movement near another solid surface.

While the theories and experimental results are well established, they are mostly on the rarefied gases. For example, the molecular picture given above is applicable strictly to ideal or rarefied gases. Some are concerned about the case of Knudsen number down to 0.01 but there have been few studies on a denser phase. Moreover, the previous theoretical studies based on the kinetic theory of dilute gases may be less useful to the dense phase. The theory predicts that the thermophoretic velocity vanishes in the limit of zero mean-free-path, which may be the case for the dense gases or liquids. For example, Eq. (1) is proportional to Knudsen number because the properties, thermal conductivities and viscosity, are proportional to the mean-free-path according to the kinetic theory of dilute gases.

$$\frac{\mu}{\rho}, \frac{k}{\rho}\sim(2RT)^{\frac{1}{2}}l \tag{2}$$

However, there does exist a finite amount of thermophoretic velocity in liquids (McNab and Meisen, 1973).

The problem may originate from the molecular model on the interaction between the particle and fluid. As a fluid phase gets denser, the configurational interaction through intermolecular potential among a collection of molecules becomes more and more important, which is missing in the kinetic theory of dilute gases. A gas molecule may always be under the influence of the potentials of other molecules or solid, and it may have less freedom to move around. A couple of gas layers may be formed permanently on the solid surface, and more layers of the diffuse character may exist on top of them. While the temperature gradient applied to the ambient fluid may not result in any pressure gradient in the case of negligible effect of convection or gravity, some pressure gradient may be developed in the interfacial region due to the influence of the solid and induce flows. Therefore, it is the interfacial region that may play a dominant role in the whole dynamics of the particle and gas system and is particular concern of the problem of thermophoresis in dense gases.

Therefore, the phenomenon may be predicted more accurately by accounting for the contribution from the intermolecular interaction through the potential in addition to the kinetic one. A couple of approaches may be relevant for the task. One may be the use of kinetic theory of dense fluids. Another may be the use of Molecular Dynamics Simulation (Han, 2005 ; Cho et al, 2002 ; Lee et al., 2002). A simpler approach may be available for dense gases if the non-equilibrium state of thermophoresis is close to equilibrium. The first equation of Born-Green-Yvon hierarchy may provide the accurate data on the fluid states in equilibrium if an adequate model of the pair correlation function is used. It was successfully applied to the coexisting states of the liquid with vapor or solid phase (Fischer and Methfessel, 1980).

In this study, a theory is developed that divides the problem of thermophoresis in dense gases in a way consistent with its characteristic scales. The Born-Green-Yvon (BGY) equation is solved for the density distribution of each smaller problem. This leads to the calculation of the pressure and viscosity distributions, and finally thermophoretic velocity of the particle. In Sec. 2, the problem is defined and the theoretical framework is derived to evaluate the velocity profile with the pressure data. Section 3 describes the computational method. Section 4 presents the results on the graphite particle in argon gas. The final section contains the conclusion.

2. Theory

2.1 Problem definition

It is considered that a rigid and non-conducting spherical particle is in a dense ambient gas (Fig. 1). The spherical particle of a radius a is pushed toward one temperature end when the temperature gradient of $(dT_\infty/d\tilde{X})$ is applied in the ambient gas. $\tilde{X}$, $\tilde{Z}$ are the global coordinates in the outer region. Since the dynamics of the interfacial region is of a primary concern and the thickness of the region is far smaller than the radius of the surface curvature, the problem may be simplified in the inner region. In the new

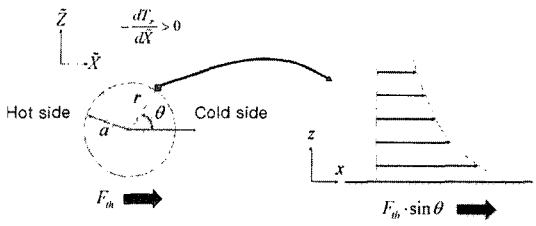

Fig. 1 Schematic of the problem

coordinates, x and z, the solid surface is considered as flat, and the lubrication approximation is used according to the smallness of the length scale in the normal direction relative to the tangential.

The flow to be developed is regarded as a creeping flow such that the effects of the inertia and convective forces are negligible. Then, with Pe, Re $\rightarrow 0$, the conservation equations are defined as follows.

$$0=-\frac{\partial P_{zz}}{\partial z}+\rho\frac{\partial \phi_s}{\partial z} \tag{3}$$

$$0=-\frac{\partial P_{xx}}{\partial x}+\mu\frac{\partial^2 u}{\partial^2 z} \tag{4}$$

$$0=\left(\frac{\partial^2}{\partial^2 x}+\frac{\partial^2}{\partial^2 z}\right)T_{g,p} \tag{5}$$

with the boundary conditions of

$$P_{xx},\ P_{zz}=P_{bulk} \qquad \text{at } z=\infty \tag{6}$$

$$u=0 \qquad \text{at } z=\infty \tag{7}$$

$$T_g=T_o+\left(\frac{dT_\infty}{d\tilde{X}}\right)r\cos\theta \qquad \text{at } r=\infty \tag{8}$$

$$T_g=T_p \qquad \text{at } r=a \tag{9}$$

$$k_g\frac{\partial T_g}{\partial r}=k_p\frac{\partial T_p}{\partial r} \qquad \text{at } r=a \tag{10}$$

The equation for conservation of mass vanishes due to the unidirectional flow structure.

2.2 Temperature and velocity field

Due to negligible influence of the convective force, Equation (5) can be decoupled from Eqs. (3) and (4) and solved first. From the spherical harmonics that satisfy the boundary conditions, it follows that

$$T_g = T_o + \left(\frac{dT_\infty}{d\tilde{X}}\right) r\cos\theta + \frac{k_g - k_p}{2k_g + k_p} a\left(\frac{dT_\infty}{d\tilde{X}}\right)\frac{a^2}{r^2}\cos\theta \quad (11)$$

$$T_p = T_o + \frac{3k_g}{2k_g + k_p}\left(\frac{dT_\infty}{d\tilde{X}}\right) r\cos\theta \quad (12)$$

In the new coordinate for the interfacial region, z $(=r-a\,;\ z \ll a)$, the temperature distribution in gas is turned into

$$T_g \simeq T_o + \left(\frac{dT_\infty}{d\tilde{X}}\right) a\cos\theta\left\{\frac{3k_g}{2k_g + k_p}\right\} \quad (13)$$

on condition that $z \ll a \cdot k_p/k_g$, which is normally satisfied.

As is explicitly expressed as P_{xx} and P_{zz} in Eqs. (3) and (4), the pressure is not of an isotropic property in the region. Therefore, some additional information for P is required for a well-posed problem. It is on the state of the dense gas. It may then be in a form similar to the ideal-gas law and must be applicable to the dense phase in the dynamics state. Due to the slowly-varying temperature distribution in the interfacial region, it may be appropriate to assume that the resulting dynamic state is still close to the equilibrium state.

$$P = P_e + O(\nabla T, \nabla u) \quad (14)$$

The velocity field can also be expanded accordingly.

$$u = u^0 + O(\nabla T, \nabla u) \quad (15)$$

Then, the static pressure P_e may be the first order solution to P in Eqs. (3) and (4). With the pressure and viscosity given, the velocity profile can readily be obtained. It is to be described how the static pressure P_e and viscosity is obtained in next subsection. The flow field has the following form

$$u(z) = \int_z^\infty d\tilde{z}\int_{\tilde{z}}^\infty d\bar{z}\frac{1}{\mu}\frac{\partial P_{xx}}{\partial x}(\bar{z}) \quad (16)$$

With

$$\frac{\partial P_{xx}}{\partial x} = \frac{\partial P_{xx}}{\partial T}\bigg|_{P_{bulk}=const.}\frac{dT}{dx} \quad (17)$$

it follows that

$$u(z) = \left[\int_z^\infty d\tilde{z}\int_{\tilde{z}}^\infty d\bar{z}\frac{1}{\mu}\frac{\partial P_{xx}}{\partial T}(\bar{z})\right]\frac{\partial T}{\partial x} \quad (18)$$

On the surface of the particle, the velocity has the value of

$$u_{slip} = u(z=0) = -b\frac{dT}{dx} \quad (19)$$

with

$$b = -\int_0^\infty d\tilde{z}\int_{\tilde{z}}^\infty d\bar{z}\frac{1}{\mu}\frac{\partial P_{xx}}{\partial T}(\bar{z}) \quad (20)$$

Since the ambient gas is stationary, the velocity on the particle surface is the velocity difference between the bulk gas and surface. Therefore, it can be regarded as a local slip velocity in the macro scale. Generally, the local slip velocity corresponds to the thermophoretic velocity of the whole particle such that

$$U_{th} = -b\frac{dT_\infty}{d\tilde{X}}\frac{3k_g}{2k_g + k_p} \quad (21)$$

(Probstein, 1994). More discussion on the derivation can be found in (Han, 2005).

2.3 Pressure tensor and viscosity

If the static pressures P_e for a set of temperatures are given, they can be put into the followings:

$$\frac{\partial P_{xx}}{\partial x} \simeq \frac{P_{xxe}(T(x_2),\ z) - P_{xxe}(T(x_1),\ z)}{x_2 - x_1} \quad (22)$$

The approximation is valid in the limit of slowing varying temperature field. This can be put into Eq. (16), which gives the velocity distribution. The static pressures can be calculated with the equilibrium density distribution, which can be obtained by solving BYG equation:

$$-k_B T\nabla_1 \ln\rho(\vec{r}_1) = \nabla_1\phi_s(\vec{r}_1) + \int d\vec{r}_2\rho(\vec{r}_2)\, g(\vec{r}_1,\ \vec{r}_2)\nabla_1\phi_{ff}(r_{12}) \quad (23)$$

This equation is equivalent to Eq. (3) if the pressure P is replaced by the static pressure P_e. The pair correlation function $g(\vec{r}_1,\ \vec{r}_2)$ can be modeled according to Fischer and Methfessel (1980).

$$g(\vec{r}_1,\ \vec{r}_2) = g^{HS}\{|r_{12}|,\ \bar{\rho}[(\vec{r}_1 + \vec{r}_2)/2]\} \quad (24)$$

with

$$\bar{\rho}(\vec{r}_1) = \frac{1}{V}\int d\vec{r}\,\rho(\vec{r}_1 + \vec{r}) \quad (25)$$

The pressure tensor is calculated by using Irving and Kirkwood formula (Irving and Kirkwood, 1950).

$$\bar{P}_T=\rho(z_1)k_BT-\frac{1}{2}\int_0^\infty dz_{12}\int_0^\infty 2\pi RdR\frac{R^2}{r_{12}}\frac{d\phi_{ff}{}^l(r_{12})}{dr_{12}}\int_0^1 da\rho(z_1-az_{12})\rho[z_1+(1-a)z_{12}]$$
$$-\frac{1}{2}kT\int_0^\infty dz_{12}\int_0^\infty 2\pi RdR\frac{R^2}{r_{12}}\delta(r_{12}-d)\int_0^1 da\rho(z_1-az_{12})\rho[z_1+(1-a)z_{12}]g^{HS}\left[d,\ \bar{\rho}\left(z_1+\frac{1}{2}z_{12}-az_{12}\right)\right] \tag{26}$$

The viscosity is also required for the interfacial region. Due to inhomogeneity in the region, the viscosity may have the value different from that in the bulk. The following relationship is used that is based on the modified Enskog theory and applicable to the weakly inhomogeneous fluids (Schrodt and Davis, 1974).

$$\mu=\frac{5}{16\sigma^2}\left(\frac{mk_BT}{\pi}\right)^{\frac{1}{2}}\left\{\frac{[1+(4\pi/15)\rho\sigma^3g^{HS}(\sigma,\rho)]^2}{g^{HS}(\sigma,\rho)}+\frac{48}{25\pi}\left(\frac{2\pi}{3\rho}\sigma^3\right)^2g^{HS}(\sigma,\rho)\right\} \tag{27}$$

3. Method

The material system of argon and graphite is considered in the simulation. The argon atoms interact with each other through the Lennard-Jones 12-6 potential.

$$u(r)=4\varepsilon\left[\left(\frac{\sigma}{r}\right)^{12}-\left(\frac{\sigma}{r}\right)^6\right] \tag{28}$$

The well-known 10-4-3 potential of graphite basal plane is used as the solid potential ϕ_s (Steele, 1973). The solid surface is assumed to be molecularly smooth so that the roughness in a larger scale is not taken account into the model.

$$\phi_s(z)=\varepsilon_{gs}\frac{2\pi qA^6}{a_s{}^*}\left[\frac{2A^6}{5(z^*)^{10}}-\frac{1}{(z^*)^4}-\frac{1}{3\Delta z^*(z^*+0.61\Delta z^*)^3}\right]a_s\sqrt{3}\,\sigma_{ss} \tag{29}$$

The numerical values for the parameters specific to argon-graphite interaction can be found in the work by Steele (1973). It can be noted that all the molecular interaction in concern are of Van der Waals kind, which is universally present in any material system. Also it is straightforward to include any other interaction for any specific material system.

BGY equation is solved through the iteration procedure (Fischer and Methfessel, 1980). Eq. (23) is transformed into

$$\rho(z_0)=\rho_\infty\exp\left\{-\frac{1}{k_BT}\left\langle\phi_s+\int d\vec{r}_1u^l(r_{01})[\rho(z_1)-\rho_\infty]\right\rangle+2\pi\int_{z_0}^\infty dz_1\int_{-d}^d dz_{12}\rho(z_2)g_{hom}^{HS}[d,\bar{\rho}((z_1+z_2)/2)]z_{11}\right\} \tag{30}$$

with

$$u^l(r)=\begin{cases}u_{\min} & \text{for } r<r_{\min},\\ u(r) & \text{for } r\geq r_{\min}.\end{cases}$$

$r_{\min}$ is the distance when u becomes the minimum value $u_{\min}$. The stepwise density profile as an initial guess is inserted into the density in the right hand side of the equation, which is then calculated to give a new profile. Unless the new profile coincides with the old one within 0.1%, the iteration continues. The Simpson's rule is used in the numerical integration in the procedure (Press et al., 1997). The bulk density must be given initially for a given pressure at each temperature. It is obtained from Eq. (30), with $\phi_s=0$, and by the Newton-Raphson procedure.

4. Results and Discussions

4.1 Density and pressure distribution

The conditions of the ambient gas are such that the temperature ranges from 1.01 to 1.31 (ε/k_B) and the bulk pressure remains 0.0140 (ε/σ^3) for the argon-graphite system. The values are chosen mainly because the fluid is in the gaseous state (Nicolas et al., 1979). Figure 2 shows the density profile for each equilibrium state. From the bulk density, Knudsen number may be estimated by the following definition.

$$Kn=1/(\sqrt{2}\rho A_Ca) \tag{31}$$

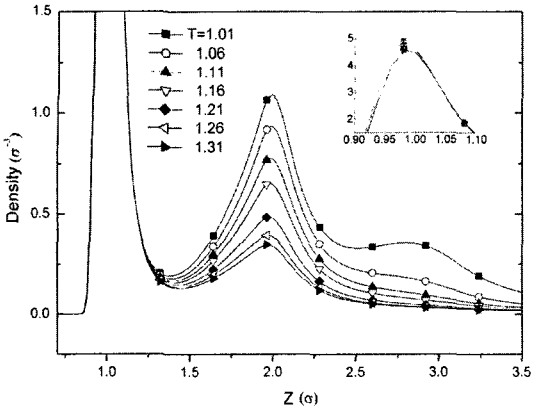

Fig. 2 Density profiles in the interfacial region

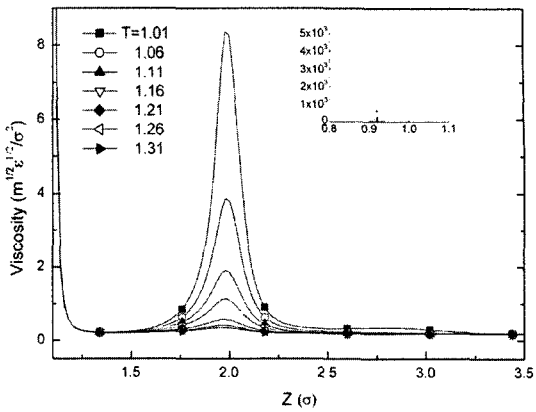

Fig. 3 Viscosity profile of the interfacial region

The following values may be applied : $\sigma=3.4\times10^{-9}$ m, $a=1.0\times10^{-6}$ m, and $\rho=1.1685\times10^{-2}\sigma^{-3}$ for T=1.3, and $\rho=1.5564\times10^{-2}\sigma^{-3}$ for T=1.01. A_C is the effective cross-sectional area for collision and may be regarded roughly as πr_i^2 where r_i is the effective range of the intermolecular force. With $r_i\approx3.5\sigma$, Kn is given as 0.0066–0.0087. In Fig. 2, it is shown that there is an absorbed layer that is clearly distinguishable and diffuse layers next to it. Due to thermal energy, the layers become of more diffuse state with a higher temperature. For the ideal gas, the density profile is given as

$$\rho=\rho_\infty \exp\left[-\frac{\phi_s}{k_B T}\right] \tag{32}$$

The bulk density of the ideal gas is linearly proportional to T^{-1} for a given state of constant pressure. The overall trends in the density of dense gases still conform to the ideal gas behavior but with some structures. For the given density profile, the viscosity can be calculated from Eq. (27) (Fig. 3). It is shown that the viscosity starts diverging in the distance of 0.05σ from the position of the density peak. This reflects much higher resistance to the shearing motion of the permanently absorbed layer. The mono-layer may have the dynamic character different from the rest of the region because it is of a dense and highly inhomogeneous phase. It may also involve the chemical or physical roughness in the molecular scale. Therefore, the approach based on Eqs. (3) ~ (6) and (16) may not be valid. Due to the high viscosity, the motion of the mono-layer is highly restricted and of relatively insignificant amount compared to the rest of the region. Therefore, this study focuses on the dynamics of only the region that excludes the mono-layer region, which is about $z>1.08$.

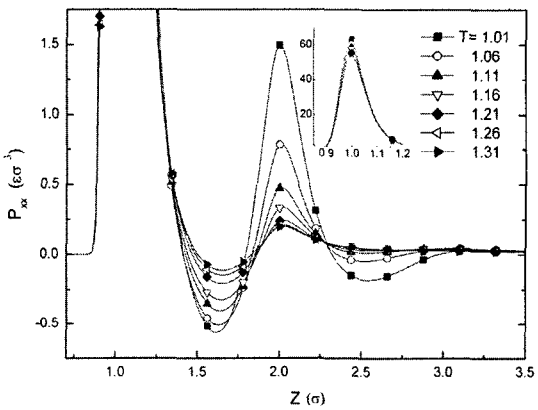

Fig. 4 Tangential pressure gradient with respect to temperature

The pressure profile tangential to the solid surface is shown in Fig. 4. The bulk pressure in all cases corresponds to 0.0140 (ε/σ^3) within +3.7% of error. However, the situation is different near the solid. Within the distance of 3σ from the solid, the pressure differences with respect to the temperatures are of considerable amount. The differences are the largest value near the position of the second diffuse layer and there also exists some oscillating behavior. The pressure profiles conform to the characteristics of the dense gas

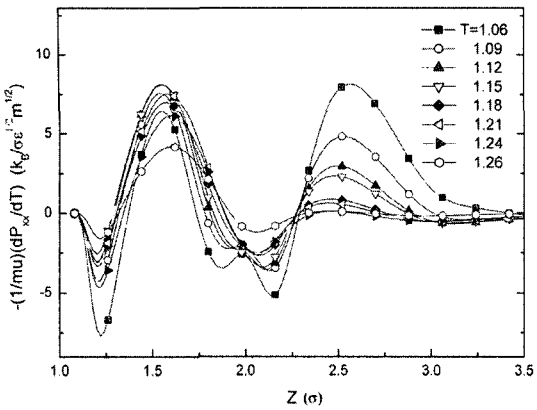

Fig. 5 Tangential pressure gradient with respect to temperature divided by viscosity

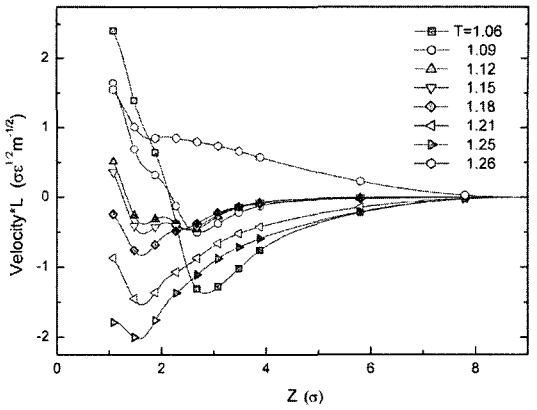

Fig. 6 Velocity profile in the interfacial region

near the solid, which is reflected in the density distribution. These pressure differences are the potential source of the flow tangential to the surface according to Eq. (18). This point may be made clear by evaluating $-\mu^{-1}(\partial P_{xx}/\partial T)$ (Fig. 5). It is shown that significant amount of pressure gradient occurs due to the temperature gradient. The pressure gradient is distributed in the region near the solid surface in a highly structured way, and it is mostly of a positive value. The latter fact corresponds to the particle movement toward the colder region according to Eq. (21).

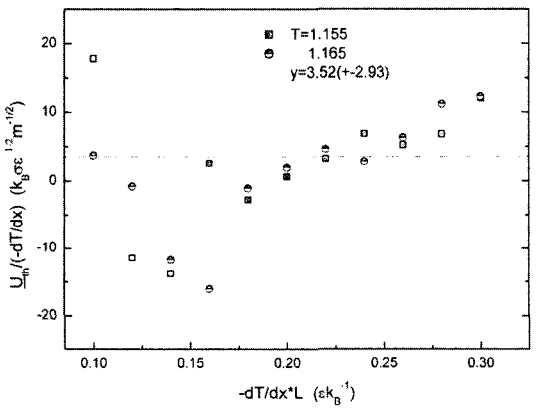

Fig. 7 Ratio of thermophoretic velocity to applied temperature gradient. $\underline{U_{th}}=U_{th}/\{3k_g/(2k_g+k_p)\}$

4.2 Thermophoretic velocity

The thermophoretic velocity profile is obtained by evaluating Eq. (16) (Fig. 6). L is the distance over which unit temperature difference is applied. The flow is developed mainly within the region next to the solid whose thickness is of about 8 molecular diameters. The velocity profile is not of a simple quadratic form but of a more complex one. From Eq. (21), the particle velocity can be derived from the local velocity on the solid surface, or local slip velocity. Figure 7 shows the behavior of the thermophoretic velocity divided by the applied temperature gradient. While the data for $-dT/dx^*L<0.175$ are rather scattered, the rest of the data clearly show that the particle velocity and applied temperature gradient are related nonlinearly. The velocity increases in a faster rate than the linear relationship as the applied temperature gradient increases. This suggests that the linear relationship commonly applied in the theories of non-equilibrium thermodynamics in the form of Eq. (1) may not be valid in the limit of dense phase of gases. This may partly come from the complex nature on how the pressure gradient and interfacial velocity are developed. The dependence of the thermophoretic velocity on temperature is shown in Fig. 8. The velocity decays with respect to temperature in a rate that is faster than T^{-1}. The data in a higher range of temperatures in the figure are scattered so that it is not easy to conclude whether the velocity changes sign or decays to zero in the limit of the highest temperature. The overall decreasing trends may result from the fact that a higher temperature reduces the influence of the solid poten-

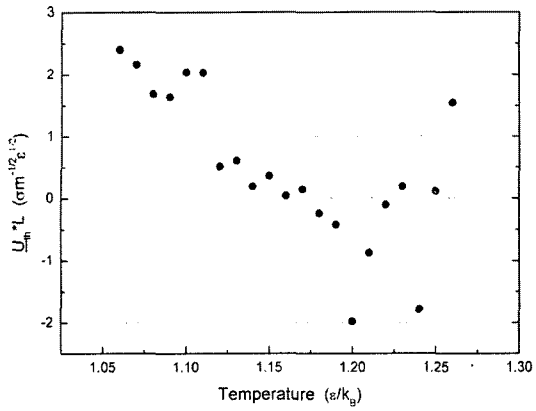

Fig. 8 Thermophoretic velocity with respect to temperature $(-dT/dx \times L=0.1)$. $\underline{U_{th}}=U_{th}/\{3 k_g/(2k_g+k_p)\}$

tial. The density and pressure gradients with respect to temperature may therefore be reduced.

Finally, it may be pointed out that two mechanisms leading to Eqs. (1) and (21) respectively are independent of each other. Therefore, they both may be effective in some intermediate range of Kn and need to be accounted for.

5. Conclusions

Thermophoresis in dense gases is investigated by using multi-scale approach and the first equation of BGY hierarchy. The conclusions of the study are in the followings;

(1) In thermophoresis of dense gases, there exists a mechanism other than the usual kinetic interaction between the fluid molecule and particle surface. The mechanism involves the intermolecular interaction through potential and has dominant effect on the particle movement. The predicted particle velocity is several orders larger than the one by the kinetic theory of rarefied gases.

(2) It is shown that the temperature gradient applied to the quiescent ambient gas induces some pressure gradient tangential to the particle surface in the interfacial region, which may be the major source of the particle movement in dense gases.

(3) The particle velocity has a nonlinear relationship with the applied temperature gradient and decays in a faster rate than T^{-1}. These deviate from the usual model dependence of $U_{th} \propto \nabla(\ln T)$, which may reflect the complex nature of the flow development in the interfacial region.

Acknowledgments

The author would like to gratefully acknowledge that this work is supported by Micro Thermal System Research Center and Samsung Corning Co.

References

Cho, S. S. and Park, S., 2002, "Molecular Dynamics Simulation of Adhesion Processes," *KSME Int. J.*, Vol. 16, No. 11, pp. 1440~1447.

Epstein, P. S., 1929, "Zur Theorie des Radiometers," *Z. Phys*, Vol. 54, pp. 537~563.

Fischer, J. and Methfessel, M., 1980, "Born-Green-Yvon Approach to the Local Densities of a Fluid at interfaces," *Phys. Rev. A.*, Vol. 22, pp. 2836~2843.

Han, M., 2005, "Thermophoresis in Liquids: a Molecular Dynamics Simulation Study," *J. Colloid Int. Sci.*, Vol. 284, Iss 1, pp. 339~348.

Irving, J. H. and Kirkwood, J. G., 1950, "The Statistical Mechanical Theory of Transport Processes. IV. The Equations of Hydrodynamics," *J. Chem. Phys.*, Vol. 18, pp. 817~829.

Lee, J., Park, S. and Kwon, O., 2002, "Characterization of Thin Liquid Films Using Molecular Dynamics Simulation," *KSME Int. J.*, Vol. 16, No. 11, pp. 1477~1484.

Maxwell, J. C. 1879, "On the Stress in Rarefied Gases Arising from Inequalities of Temperature," *Philos. Trans. R. Soc.*, Part I, Vol. 2, pp. 255~286.

McNab, G. S. and Meisen, A., 1973, "Thermophoresis in Liquids," *J. Coll. Int. Sci.*, Vol. 44, pp. 399~346.

Nicolas, J. J., Gubbins, K. E., Streett, W. B. and Tildesley, D. J., 1979, "Equation of State for the Lennard-Jones Fluid," *Mol. Phys.*, Vol. 37, pp. 1429~1454.

Press, W. H., Teukolsky, S. A., Vetterling, W. T. and Flannery, B. P., 1997, *Numerical Recipes*

in C : The Art of Scientific Computing, Cambridge University Press, Cambridge.

Probstein, R. F., 1994, *Physicochemical Hydrodynamics : An Introduction*, John Wiley & Sons, New York.

Schrodt, I. B. and Davis, H. T., 1971, "Kinetic Theory of Dense Fluids," *J. Chem. Phys.*, Vol. 61, pp. 323~329.

Sone, Y., 2000, "Flow Induced by Temperature Fields in a Rarefied Gas and Their Ghost Effect on the Behavior of a Gas in the Continuum Limit," *Ann. Rev. Fluid Mech.*, Vol. 32, pp. 779~811.

Steele, W. A., 1973, "The Physical Interaction of Gases with Crystalline Solids. I. Gas-solid Energies and Properties of Isolated Adsorbed Atoms," *Surf. Sci.*, Vol. 36, pp. 327~352.

Zheng, F., 2002, "Thermophoresis of Spherical and Non-spherical Particles : a Review of Theories and Experiments," *Adv. Coll. Interf. Sci.*, Vol. 97, pp. 255~278.